Asian Journal of Chemistry; Vol. 38, No. 2 (2026), 411-416
ASIAN JOURNAL OF CHEMISTRY
https://doi.org/10.14233/ajchem.2026.35020

Synthesis, Characterisation, Molecular Docking and Biological Response of Some New Xylenol Analogues

A. SARAH GRACE[1], L. THANGAVELU[2], M. RUBASRIGAYATHRI[3], T. VIJAYALAKSHMI[3], S.A. SRI HARISH[3], T.A. SHIREEN FARZHANA[4], M. PAVITHRA[4] and S. FULORIA[1,*]

[1]Pharmaceutical Chemistry Unit, Faculty of Pharmacy, AIMST University, Bedong 08100, Kedah, Malaysia
[2]Center for Global Health Research, Saveetha Medical College, Saveetha Institute of Medical and Technical Sciences, Chennai-600077, India
[3]Department of Biochemistry, Saveetha Medical College, Saveetha Institute of Medical and Technical Sciences, Saveetha University, Chennai-600077, India
[4]Department of Microbiology, Saveetha Medical College, Saveetha Institute of Medical and Technical Sciences, Saveetha University, Chennai-600077, India

*Corresponding author: E-mail: shivkanya_fuloria@aimst.edu.my

Received: 7 October 2025 *Accepted*: 5 January 2026 *Published online*: 31 January 2026 AJC-22258

Owing to the versatile biochemical properties of xylenols, the current study was intended to synthesize and characterize some new xylenol analogues (NXAs). The NXAs were evaluated for *in vitro* inhibitory activity against osteomyelitis triggering pathogens (*S. aureus* and *E. coli*), followed by *in silico* AutoDock studies against their key proteins. The NXAs synthesis involved substituted xylenol (**1**) esterification, hydrazination and subsequent treatment with 4-aminoacetophenone to yield intermediate N-(1-(4-aminophenyl)ethylidene)-2-(2,3-dimethylphenoxy)acetohydrazide (**4**), which was further treated with different aromatic aldehydes to yield *N*-(1-(4-((substituted benzylidene)-amino)phenyl)ethylidene)-2-(2,3-dimethylphenoxy)acetohydrazide (**5a-g**) following condensation reaction. The synthesised NXAs were characterised using ATR-IR, ^{1}H NMR, ^{13}C NMR and mass spectrometry. The characterised NXAs were further evaluated for their *in vitro* inhibitory activity against the osteomyelitis-triggering pathogens *S. aureus* and *E. coli*, followed by *in silico* binding affinity studies using AutoDock against their respective key proteins, DNA gyrase B (PDB ID: 4URM) and UDP-N-acetylglucosamine enolpyruvyl transferase (PDB ID: 1UAE). Present investigation concludes synthesis and characterisation success of NXAs and high inhibitory potential against osteomyelitis triggering pathogens and binding affinity with their respective proteins 4URM and 1UAE. Present study recommends that in future the synthesised NXAs of this study should be further subjected to preclinical evaluation for osteomyelitis treatment.

Keywords: Azomethine, Xylenols, Docking studies, Biological activities.

INTRODUCTION

Versatile biochemical properties of phenols make them privileged molecules in medicinal chemistry research [1]. Evidence suggests xylenol derived compounds as a valuable lead structure bearing strong antibacterial, antifungal, anti-cancer and anti-inflammatory properties [2]. The presence of hydroxyl group in xylenols is known to enable hydrogen bonding, redox activity and proton donation, which elicits the anti-inflammatory potential of the molecule [2,3]. Whereas, methyl groups of xylenols are known to offers the lipophilicity, which improves the membrane permeability and target interaction of any organic scaffold [4]. The structural simplicity, tunable electronic properties and synthetic flexibility of xylenols allow their conversion into potential esters, ethers and Schiff bases [5,6].

Current era has witnessed high incidence of infections induced osteomyelitis in trauma, post-surgical cases, diabetic patients and populations with poor hygiene and healthcare [7,8]. Several studies reported synthesis of various phenols and xylenol derivatives, however their safety, mechanism and resistance were the major problems [9-11]. Hence development of some new scaffolds is important for investigators. Reports highlight that insertion of azomethine group in organic moieties improves their biological activity, physico-chemical properties and safety [12]. Facts suggest that azomethine ability for H-bonding and π-stacking in bio-targets offers high anti-microbial activities [13,14].

In modern drug discovery, the development of new scaffolds by molecular docking through AutoDock Vina is one of the key avenues [15]. Previous studies [16,17] have demonstrated that infections caused by *Staphylococcus aureus* and *Escherichia coli*, two key pathogens implicated in osteomyelitis, can be effectively addressed by targeting essential bacterial enzymes such as DNA gyrase B (PDB ID: 4URM) in *S. aureus* and UDP-N-acetylglucosamine enolpyruvyl transferase (PDB ID: 1UAE) in *E. coli* [18,19]. Hence based evidences on xylenols, osteomyelitis inducing bacteria (*S. aureus* and *E. coli*), ongoing synthesis and problems of current scaffolds and the potency of xylenols and azomethines were the motivation to perform synthesis, characterisation, docking analysis and inhibitory activity of some new xylenol analogues (NXAs) against osteomyelitis triggering pathogens.

EXPERIMENTAL

All chemical and biological materials were obtained from Qrec Chemicals, HmbG®, Merck KGaA and Sigma-Aldrich. The NXAs synthesised were structurally elucidated based on ^{1}H and ^{13}C NMR data obtained on Bruker instrument at 400 MHz. Infrared spectra were acquired using Perkin-Elmer ATR-FTIR instrument, whereas mass analysis was done using direct infusion ion-trap mass spectrometer. The purity of NXAs was assessed by determining melting points using an open-capillary method.

Synthesis of *N*-(1-(4-aminophenyl)ethylidene)-2-(2,3-dimethylphenoxy)acetohydrazide (4): Compound **NXA 4** was synthesised as per standard procedure [20,21], briefly, the reaction mixture of compound **3** (synthesised by hydrazination of ester derivative **2** of compound **1**) and 4-aminoacetophenone (0.0001 M) in absolute ethyl alcohol was refluxed for 8 h. To monitor the reaction and purity of **NXA 4**, the TLC experiment was performed using methanol:chloroform in 9:1 ratio. The resultant compound was recrystallised using methyl alcohol to obtain cystalline **NXA 4** as yellow product. Yield: 78%, R_f: 0.49, m.p.: 146 ºC; IR (KBr, ν_{max}, cm^{-1}): 3258 (N–H), 3026 (aryl C–H), 2924 (alkyl C–H), 1679 (C=O), 1604 (C=N), 1472 (C=C); ^{1}H NMR (400 MHz, DMSO-d_6, δ ppm): 1.1 (s, 3H, CH_3), 2.26 (s, 3H, CH_3), 2.46 (s, 3H, CH_3), 4.88 (s, 2H, OCH_2), 5.87 (s, 2H, NH_2), 6.49-7.52 (m, 7H, Ar-H), 9.63 (s, 1H, NH); ^{13}C NMR (400 MHz, DMSO-d_6, δ ppm): 11 (CH_3), 18 (CH_3), 22 (CH_3), 69 (CH_2), 111, 116, 121, 124, 128, 132, 138, 150 (aryl-C), 158 (aryl-C–O), 169 (N–N=C), 191 (O=C); Mass (*m/z*): 311 (parent ion).

Synthesis of *N*-(1-(4-(benzylideneamino)phenyl)ethylidene)-2-(2,3-dimethylphenoxy)acetohydrazide (5a-g): The synthesis of **NXAs 5a-g** was executed as per standard procedure [22]. Briefly, the reaction mixture of **NXA 4** and benzaldehyde at concentration of 0.0001 M (equimolar) in absolute ethyl alcohol was refluxed for 8 h. To monitor the reaction and purity of **NXA 5a**, the TLC experiment was performed using methanol: chloroform in 8:2 ratio. The resultant compound was recrystallised using methyl alcohol to obtain pure **NXA 5a** (**Scheme-I**). Similarly, other NXAs **5b-g** were also synthesized by following the same procedure.

***N*-(1-(4-(Benzylideneamino)phenyl)ethylidene)-2-(2,3-dimethylphenoxy)acetohydrazide (5a):** White, yield: 80%, R_f: 0.58, m.p.: 134 ºC; IR (KBr, ν_{max}, cm^{-1}): 3254 (N–H), 3032 (aryl C–H), 2927 (alkyl C–H), 1677 (C=O), 1609 (C=N), 1461 (C=C); ^{1}H NMR (400 MHz, DMSO-d_6, δ ppm): 1.12 (s, 3H, CH_3), 2.24 (s, 3H, CH_3), 2.45 (s, 3H, CH_3), 4.86 (s, 2H, OCH_2), 6.49-7.63 (m, 12H, Ar-H), 8.40 (s, 1H, NH) and 9.61 (s, 1H, N=CH); ^{13}C NMR (400 MHz, DMSO-d_6, δ ppm): 12 (CH_3), 18 (CH_3), 21 (CH_3), 70 (CH_2), 111, 118, 121, 124, 129, 130, 132, 138, 150, 155 (aryl-C), 158 (aryl-C–O), 161 (N=C), 169 (N–N=C), 191 (O=C); Mass (*m/z*): 399 (parent ion).

***N*-(1-(4-(4-Chlorobenzylideneamino)phenyl)ethylidene)-2-(2,3-dimethylphenoxy)acetohydrazide (5b):** White, yield: 90%, R_f: 0.45, m.p.: 158 ºC; IR (KBr, ν_{max}, cm^{-1}): 3253 (N–H), 3030 (aryl C–H), 2921 (aliphatic C–H), 1674 (C=O), 1610 (C=N), 1462 (C=C); ^{1}H NMR (400 MHz, DMSO-d_6, δ ppm): 1.12 (s, 3H, CH_3), 2.22 (s, 3H, CH_3), 2.44 (s, 3H, CH_3), 4.87 (s, 2H, OCH_2), 6.46-7.58 (m, 11H, Ar-H), 8.42 (s, 1H, NH), 9.64 (s, 1H, N=CH); ^{13}C NMR (400 MHz, DMSO-d_6, δ ppm): 11 (CH_3), 17 (CH_3), 20 (CH_3), 72 (CH_2), 111, 117, 120, 123, 128, 130, 133, 137, 150, 156 (aryl-C), 159 (aryl-C–O), 162 (N=C), 169 (N–N=C), 192 (O=C); Mass (*m/z*): 433 (parent ion).

***N*-(1-(4-(4-(Dimethylamino)benzylideneamino)phenyl)-ethylidene)-2-(2,3-dimethylphenoxy)acetohydrazide (5c):** Orange, yield: 87%, R_f: 0.49, m.p.: 149 ºC; IR (KBr, ν_{max}, cm^{-1}): 3251 (N–H), 3034 (aryl C–H), 2922 (alkyl C–H), 1670 (C=O), 1605 (C=N), 1468 (C=C); ^{1}H NMR (400 MHz, DMSO-d_6, δ ppm): 1.11 (s, 3H, CH_3), 2.22 (s, 3H, CH_3), 2.44 (s, 3H, CH_3), 2.98 (s, 6H, $(NCH_3)_2$), 4.89 (s, 2H, OCH_2), 6.46-7.49 (m, 11H, aryl-H), 8.41 (s, 1H, NH) and 9.69 (s, 1H, N=CH); ^{13}C NMR (400 MHz, DMSO-d_6, δ ppm): 11 (CH_3), 17 (CH_3), 20 (CH_3), 59 ($N\text{-}CH_3)_2$, 71 (CH_2), 111, 116, 119, 124, 128, 131, 134, 138, 152 (aryl-C), 159 (aryl-C–O), 162 (N=C), 168 (N–N=C), 191 (O=C); Mass (*m/z*): 442 (parent ion).

***N*-(1-(4-(4-Hydroxybenzylideneamino)phenyl)ethylidene)-2-(2,3-dimethylphenoxy)acetohydrazide (5d):** Yellow, yield: 85%, R_f: 0.55, m.p.: 146 ºC; IR (KBr, ν_{max}, cm^{-1}): 3257 (N–H), 3033 (aryl C–H), 2924 (alkyl C–H), 1672 (C=O), 1608 (C=N), 1469 (C=C); ^{1}H NMR (400 MHz, DMSO-d_6, δ ppm): 1.12 (s, 3H, CH_3), 2.20 (s, 3H, CH_3), 2.42 (s, 3H, CH_3), 4.88 (s, 2H, OCH_2), 6.46-7.66 (m, 11H, aryl-H), 7.71 (brs, 1H, OH), 8.44 (s, 1H, NH), 9.63 (s, 1H, N=CH); ^{13}C NMR (400 MHz, DMSO-d_6, δ ppm): 12 (CH_3), 16 (CH_3), 21 (CH_3), 70 (CH_2), 111, 116, 118, 125, 128, 130, 136, 139, 142 (aryl-C), 158 (aryl-C–O), 161 (N=C), 167 (N–N=C), 190 (O=C); Mass (*m/z*): 415 (parent ion peak).

***N*-(1-(4-(4-Methoxybenzylideneamino)phenyl)ethylidene)-2-(2,3-dimethylphenoxy)acetohydrazide (5e):** White, yield: 81%, R_f: 0.58, m.p.: 162 ºC; IR (KBr, ν_{max}, cm^{-1}): 3256 (N–H), 3039 (aryl C–H), 2929 (alkyl C–H), 1673 (C=O), 1609 (C=N), 1462 (C=C); ^{1}H NMR (400 MHz, DMSO-d_6, δ ppm): 1.12 (s, 3H, CH_3), 2.20 (s, 3H, CH_3), 2.41 (s, 3H, CH_3), 3.81 (s, 3H, OCH_3), 4.86 (s, 2H, OCH_2), 6.46-7.39 (m, 11H, aryl-H), 8.40 (s, 1H, NH), 9.66 (s, 1H, N=CH); ^{13}C NMR (400 MHz, DMSO-d_6, δ ppm): 11 (CH_3), 17 (CH_3), 20 (CH_3), 63 ($O\text{-}CH_3$), 71 (CH_2), 111, 116, 119, 124, 128, 131, 134, 138, 152 (aryl-C), 158 (aryl-C–O), 161 (N=C), 169 (N–N=C), 192 (O=C); Mass (*m/z*): 429 (parent ion).

***N*-(1-(4-(4-Aminobenzylideneamino)phenyl)ethylidene)-2-(2,3-dimethylphenoxy)acetohydrazide (5e):** Light yellow,

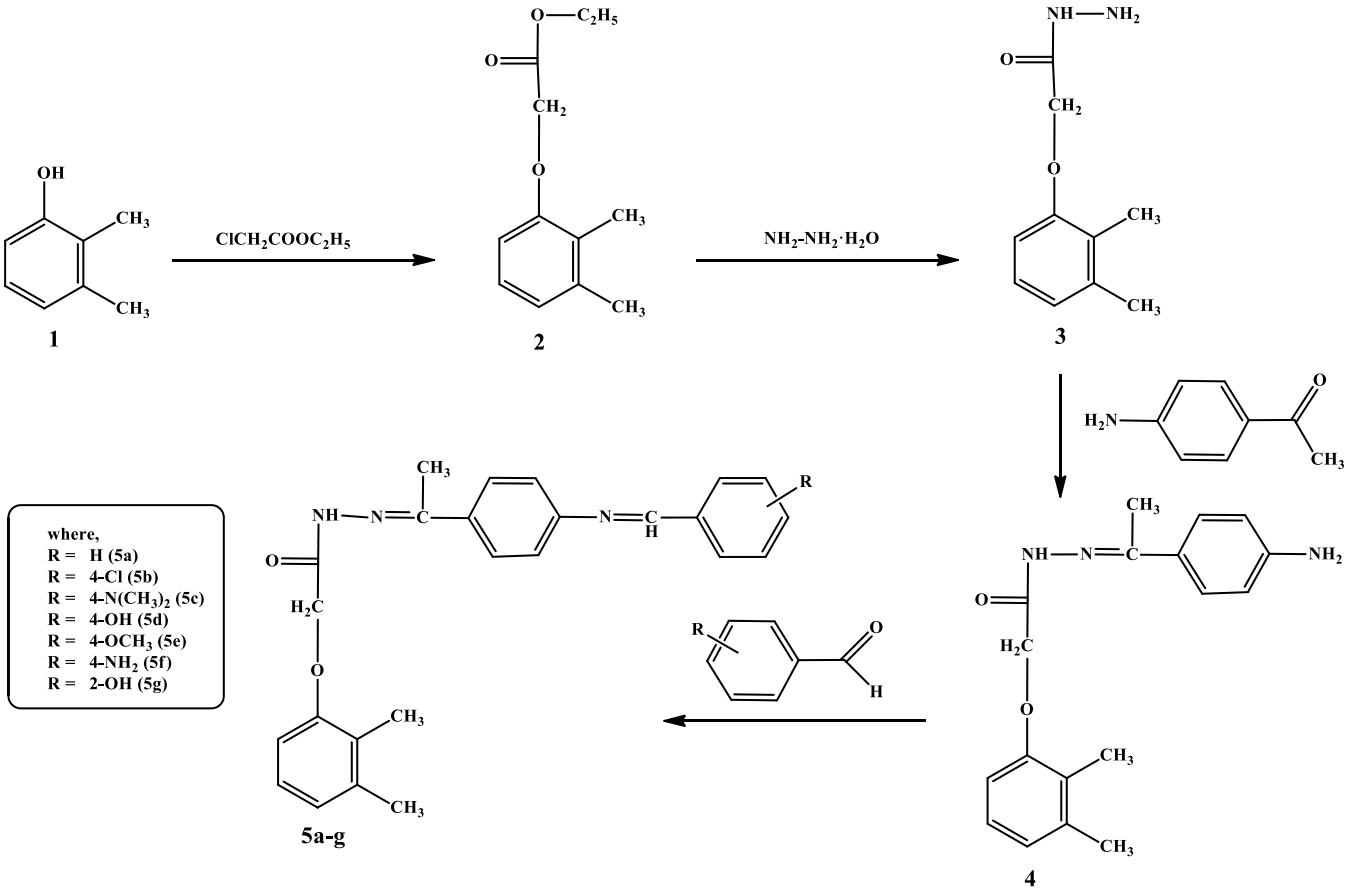

Scheme-I: Synthesis of novel xylenol derivatives (**5a-g**)

yield: 84%, R_f: 0.43, m.p.: 159 ºC; IR (KBr, ν_{max}, cm^{-1}): 3251 (N–H), 3033 (aryl C–H), 2925 (alkyl C–H), 1672 (C=O), 1610 (C=N), 1465 (C=C); ^{1}H NMR (400 MHz, DMSO-d_6, δ ppm): 1.11 (s, 3H, CH_3), 2.21 (s, 3H, CH_3), 2.42 (s, 3H, CH_3), 4.85 (s, 2H, OCH_2), 6.46-7.36 (m, 11H, aryl-H), 8.41 (s, 1H, NH) and 9.64 (s, 1H, N=CH); ^{13}C NMR (400 MHz, DMSO-d_6, δ ppm): 11 (CH_3), 16 (CH_3), 21 (CH_3), 73 (CH_2), 112, 115, 118, 123, 127, 132, 135, 139, 151 (aryl-C), 159 (aryl-C–O), 162 (N=C), 170 (N–N=C), 191 (O=C); Mass (*m/z*): 415 (parent ion).

N-(1-(4-(2-Hydroxybenzylideneamino)phenyl)ethylidene)-2-(2,3-dimethylphenoxy)acetohydrazide (5g): White, yield: 79%, R_f: 0.51, m.p.: 155 ºC; IR (KBr, ν_{max}, cm^{-1}): 3252 (N–H), 3034 (aryl C–H), 2928 (alkyl C–H), 1676 (C=O), 1610 (C=N), 1465 (C=C); ^{1}H NMR (400 MHz, DMSO-d_6, δ ppm): 1.11 (s, 3H, CH_3), 2.21 (s, 3H, CH_3), 2.43 (s, 3H, CH_3), 4.85 (s, 2H, OCH_2), 6.46-7.64 (m, 11H, aryl-H), 7.70 (brs, 1H, OH), 8.43 (s, 1H, NH) and 9.62 (s, 1H, N=CH); ^{13}C NMR (400 MHz, DMSO-d_6, δ ppm): 11 (CH_3), 17 (CH_3), 22 (CH_3), 72 (CH_2), 111, 115, 118, 124, 128, 131, 135, 138, 141 (aryl-C), 156 (aryl-C–O), 162 (N=C), 168 (N–N=C), 192 (O=C); Mass (*m/z*): 415 (parent ion).

Molecular docking: Synthesised NXAs were evaluated for their biochemical properties through molecular docking analysis (MDA) with target proteins, namely: 4URM of *S. aureus* and 1UAE of *E. coli* using AutoDock [23-25]. In brief, molecular docking analysis (MDA) of the NXAs was performed to investigate their binding interactions and orientation within the active sites of the selected target proteins, through system of 16 GB RAM and Intel® Core™ i7 processor. The workflow encompassed protein preprocessing, design of NXAs and their conversion into compatible file formats employing Discovery Studio, AutoDock v4.2.7, MGLTools v1.5.7, ChemDraw and OpenBabel [25,26]. Two-dimensional chemical structures of all NXAs were initially generated using ChemSketch and subsequently transformed into their corresponding three-dimensional conformations. The generated NXAs were geometrically optimised and subjected to energy minimisation prior to docking simulations [27]. Three-dimensional coordinates of the target proteins (PDB IDs: 4URM and 1UAE) were downloaded from RCSB Protein Data Bank. Protein preparation was performed by Discovery Studio Visualizer, involving deletion of crystallographic water molecules and heteroatoms, followed by the incorporation of polar hydrogens and assignment of charge through Molecular Graphics Laboratory tools. Grid box configuration was defined using AutoDock v4.2.7, docking simulations was done with AutoDock Vina (version 1.1.2). The resultant binding poses were analysed using Discovery Studio Visualizer [28].

Antibacterial activity: All the synthesised compounds were subsequently screened for *in vitro* inhibitory activity against *S. aureus* and *E. coli* employing the standard disc diffusion technique [29]. In brief, freshly grown bacterial suspensions were uniformly spread over Mueller-Hinton agar (MHA) plates. The sterilised paper discs (6 mm diameter) were indi-

vidually loaded with each compound at 100 µg/mL concentration, prepared in DMSO (0.5%) and placed on inoculated agar surface of MHA plate. Plates were then incubated at 37 ºC for 24 h, followed by assessment of antibacterial activity by recording inhibition zone (mm) diameter surrounding each disc. In this study, the *para*-chloro *meta*-xylenol (PCMX) was used as standard.

RESULTS AND DISCUSSION

The synthesis and characterization of synthesized substituted xylenol was found to be consistent with earlier reported literature [28,30]. ATR-FTIR spectral analysis of **NXA 4** and **5a-g** revealed the characteristic absorption bands corresponding to N–H stretching (3258-3251 cm^{-1}), aromatic =C–H stretching (3039-3026 cm^{-1}), aliphatic C–H stretching (2929-2921 cm^{-1}) and carbonyl (C=O) functionalities (1679-1670 cm^{-1}), providing the preliminary structural confirmation. The spectral data of these NXAs agreed with the previously studies [20,22]. Furthermore, the ^{1}H NMR spectra of **NXA 5a-g** exhibited characteristic signal between δ 9.61-9.69 ppm, indicating successful synthesis of **NXA 5a-g**. The proposed chemical structures of synthesised NXAs were also supported with ^{13}C NMR and mass analysis data.

Molecular docking studies: The molecular docking analysis (MDA) evaluated the binding strength and interaction of NXAs with target proteins 4URM and 1UAE using AutoDock platform [31]. Previous MDA study reported favourable binding interactions of 3-methyl-1,4-diarylazetidin-2-one derivatives and *S. aureus* DNA gyrase subunit B (4URM) [32] and highlighted suitability of this 4URM for inhibitor designing. Similarly, present MDA study also demonstrated that all NXAs listed in Table-1, including compounds **2**, **3**, **4** and **5a-g**, exhibits good binding affinities on active sites of 4URM and 1UAE of *S. aureus* and *E. coli* respectively, offering much higher docking score than *para*-chloro-*meta*-xylenol (PCMX). Among the tested compounds, **NXAs 5c** and **5f** achieved the most favourable binding affinity toward 4URM (with docking score of -9.2 Kcal/mol) and 1UAE (with docking score of -10.6 Kcal/mol) is much higher than standard PCMX. Apart from it, **NXAs 5c** and **5f** exhibited stable and well aligned conformations in active pockets of 4URM and 1UAE, respectively. Literary evidence highlights that the hydrogen bond interaction between ligand and amino acid residues of any protein supports stabilisation of complex on one hand and overall binding strength on the other hand [33].

TABLE-1
DOCKING SCORE OF SYNTHESIZED NXAs AGAINST PROTEINS 4URM AND 1UAE

Compound	Docking score (kcal/mol)	
	4URM	1UAE
1	-5.2	-5.1
2	-6.5	-6.3
3	-7.6	-6.9
4	-7.8	-8.7
5a	-8.7	-9.6
5b	-7.9	-9.7
5c	-9.2	-9.0
5d	-8.5	-10.4
5e	-7.9	-9.1
5f	-9.0	-10.6
5g	-8.9	-10.5
Chloroxylenol	-5.5	-5.3
Ligand	–	–

The 2D interaction diagram presented in Fig. 1a, reveals the stable fitting of **NXA 5c** in active site of 4URM, which supports its strong binding. As per the 2D image, it is revealed that in **NXA 5c** molecule, the N-atom of hydrazone group undergoes electrostatic interaction with glutamic acid at position 58 in Chain A. The conventional hydrogen bonding between O-atom of carbonyl group with threonine at position 173 also occurs in chain A. The hydrogen bond interactions provide substantial strength, ligand stability (in binding pocket), ligand alignment, retention at active site and finally improves binding efficiency [32]. These interactions indicate efficient occu-

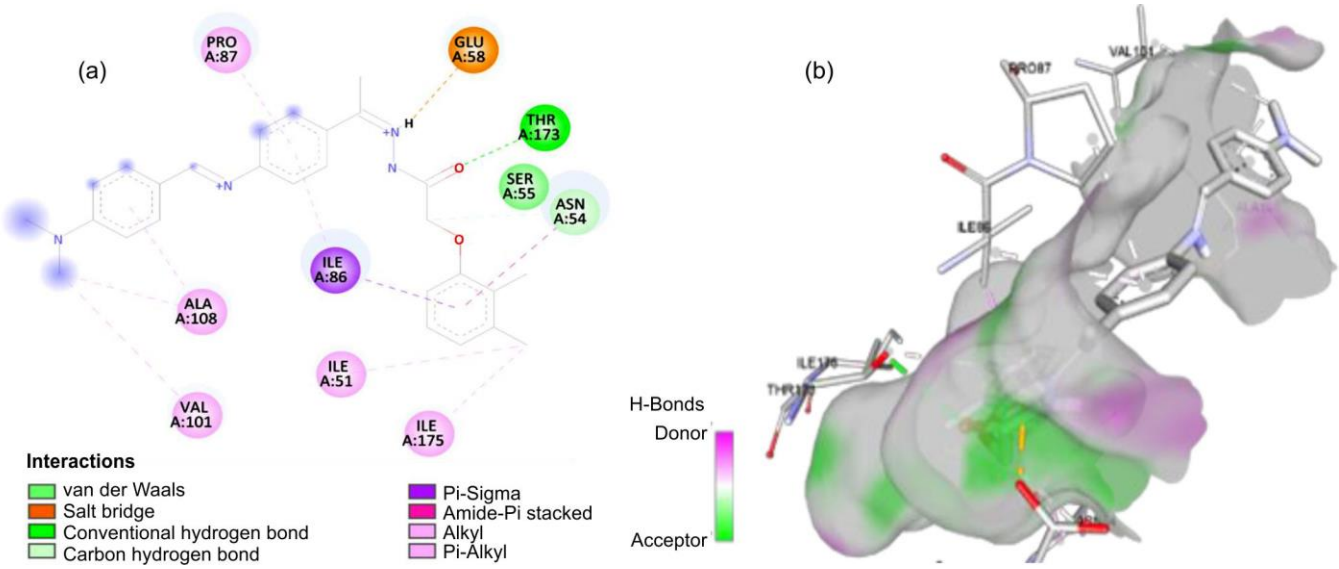

Fig. 1. (a) 2D and (b) 3D images of **NXA 5c** with 4URM

pation of active site of 4URM by **NXA 5c**, thereby suggests its potential as inhibitor of DNA gyrase of *S. aureus*. The 3D pose of docking conformation of the **NXA 5c**-4URM complex (Fig. 1b) further indicates a strong binding interaction, thereby supporting the inhibitory potential of **NXA 5c** against *S. aureus*.

Similarly, the 2D interaction pose (Fig. 2a), reveals stable fitting of **NXA 5f** in active site of 1UAE, which supports its strong binding. As per the 2D image, it is revealed that in **NXA 5f** molecule the N-atom of hydrazone group undergoes electrostatic interaction with glutamic acid at position 188 and with asparagine at position 305 in Chain A. The conventional hydrogen-bond interactions were observed between the carbonyl oxygen and Arg232, the amide NH_2 hydrogens with Asn123 and Pro121, the imino nitrogen with Val161, and the ether oxygen with Asn123 within chain A. These interactions indicate efficient occupation of active site of 1UAE by **NXA 5f**, thereby suggests its potential as inhibitor of *E. coli.* The 3D docking pose of **NXA 5f** with 1UAE (Fig. 2b) confirmed the strong binding interactions, supporting its potential inhibitory activity against *Escherichia coli*.

Biology: The inhibitory activity of all NXAs (**4** and **5a-g**) including compounds **2** and **3** against osteomyelitis triggering pathogens *S. aureus* and *E. coli* was assessed by disc diffusion assay at 100 µg/mL test concentration prepared in DMSO solvent (0.5%). Among all, compound **NAXs 5c** and **5f** demonstrated high inhibition potential against *S. aureus* and *E. coli*, respectively (Table-2). The results are found to be in good agreement with the previous studies [34-36], which further supports the inhibition potential of these NXAs against the tested osteomyelitis pathogens.

TABLE-2
ANTIMICROBIAL ACTIVITY DATA OF SYNTHESIZED COMPOUNDS NXA

Compound	Zone of inhibition (mm)	
	S. aureus	*E. coli*
2	18	16
3	15	14
4	23	22
5a	19	17
5b	20	17
5c	23	21
5d	21	20
5e	18	15
5f	24	22
5g	21	19
PCMX	25	23

Conclusion

The present study successfully synthesised a series of novel xylenol analogues (NXAs) and confirmed their structures through IR, ^{1}H & ^{13}C NMR and mass spectrometric data. The results demonstrated that all NXAs exhibited favour-able molecular docking performance, with compounds **5c** and **5f** to exhibit strongest binding affinities toward 4URM and 1UAE, the key targets associated with osteomyelitis related infections. The *in silico* outcomes were further established by *in vitro* inhibition assays against *S. aureus* and *E. coli*. Based on the results of this research, present study suggests that further preclinical evaluations are needed to further establish the inhibitory potential of NXAs in osteomyelitis treatment.

ACKNOWLEDGEMENTS

The authors are thankful to the respective departments of AIMST university, Malaysia and Saveetha University, India for their support in successful completion of this study.

CONFLICT OF INTEREST

The authors declare that there is no conflict of interests regarding the publication of this article.

DECLARATION OF AI-ASSISTED TECHNOLOGIES

The authors declare that no AI tools were used in the preparation or writing of this research article.

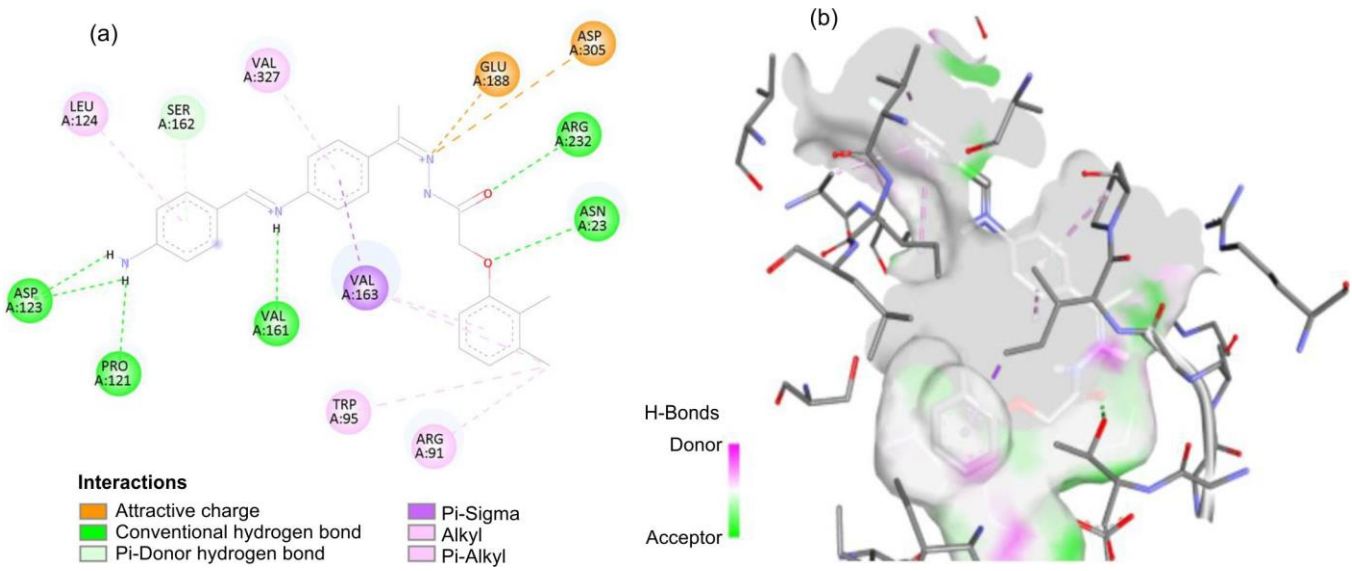

Fig. 2. (a) 2D and (b) 3D images of **NXA 5f** with 1UAE

REFERENCES

1. K.A. Scott, P.B. Cox and J.T. Njardarson, *J. Med. Chem.*, **65**, 7044 (2022); https://doi.org/10.1021/acs.jmedchem.2c00223
2. W. Sun and M.H. Shahrajabian, *Molecules*, **28**, 1845 (2023); https://doi.org/10.3390/molecules28041845
3. W. Xu, Z. Lin, C. Cortez-Jugo, G.G. Qiao and F. Caruso, *Angew. Chem. Int. Ed.*, **64**, e202423654 (2025); https://doi.org/10.1002/anie.202423654
4. İ. Gulcin, *Arch. Toxicol.*, **99**, 1893 (2025); https://doi.org/10.1007/s00204-025-03997-2
5. W. Sun and M.H. Shahrajabian, *Molecules*, **28**, 1845 (2023); https://doi.org/10.3390/molecules28041845
6. R. Retnosari, A.H. Ali, S. Zainalabidin, A. Ugusman, N. Oka and J. Latip, *Bioorg. Med. Chem. Lett.*, **109**, 129826 (2024); https://doi.org/10.1016/j.bmcl.2024.129826
7. S. Mondal, M. Lodh, S. Sahoo, K. Paul, D. Biswas, C. Krishna, A. Parida, A. Ganguly and R. DasGupta, *Sci. Rep.*, **15**, 2576 (2025); https://doi.org/10.1038/s41598-025-86013-y
8. R. Da Ros, R. Assaloni, A. Michelli, B. Brunato and C. Miranda, *Antibiotics*, **13**, 1142 (2024); https://doi.org/10.3390/antibiotics13121142
9. M.Y. Chang, Y.C. Wang, M.J. Iqbal, D.D. Ejeta and C.H. Lin, *Polymer*, **339**, 129191 (2025); https://doi.org/10.1016/j.polymer.2025.129191
10. M.C. Lourenço, T. Nascimento, P.J. Filho, A.C. Marques and M. Ramos-Andrés, *Int. J. Mol. Sci.*, **26**, 4872 (2025); https://doi.org/10.3390/ijms26104872
11. J. Wu and M.C. Kozlowski, *ACS Catal.*, **12**, 6532 (2022); https://doi.org/10.1021/acscatal.2c00318
12. H. Abbo, D.E. Holman, M.D. Hendricks, C.A. Salubi, M. Keyster and S. Titinchi, *Results Chem.*, **13**, 101986 (2025); https://doi.org/10.1016/j.rechem.2024.101986
13. H. Azevedo-Barbosa, B.P. do Vale, G. Guidolin Rossi, F. dos Santos Siqueira, K. Bordignon Guterres, M.M. de Campos, T. Dos Santos, J. Anthony Hawkes, D. Ferreira Dias, S. Neiva Lavorato, T.B. de Souza and D. Teixeira Carvalho, *Chem. Biodivers.*, **18**, e2100066 (2021); https://doi.org/10.1002/cbdv.202100066
14. A. Bouzaheur, A. Bouchoucha, K. Si Larbi and S. Zaater, *J. Mol. Struct.*, **1261**, 132811 (2022); https://doi.org/10.1016/j.molstruc.2022.132811
15. A.K. Yadav, N. Singh, M. Silwal, A. Adhikari and P.N. Yadav, *Results Chem.*, **11**, 101794 (2024); https://doi.org/10.1016/j.rechem.2024.101794
16. M. Song, J. Sun, K. Lv, J. Li, J. Shi and Y. Xu, *Clin. Exp. Med.*, **25**, 131 (2025); https://doi.org/10.1007/s10238-025-01595-1
17. T. Luu, G. Reid and B. Lavery, *IDCases*, **27**, e01381 (2022); https://doi.org/10.1016/j.idcr.2022.e01381
18. B.O. Aljohny, A. Rauf, Y. Anwar, S. Naz and A. Wadood, *ACS Omega*, **6**, 5878 (2021); https://doi.org/10.1021/acsomega.0c06297
19. M.A. Abbas, G.Y. Lee, S.A. Sayem, S.J. Lee and S.C. Park, *Antioxidants*, **14**, 1114 (2025); https://doi.org/10.3390/antiox14091114
20. A.J.M. Xavier, M.A. Raj and J.M. Marie, *J. Chem. Pharm. Res.*, **4**, 669 (2012).
21. M. Shaharyar, A. Mazumder, Salahuddin, R. Garg and R.D. Pandey, *Arab. J. Chem.*, **9**, S342 (2016); https://doi.org/10.1016/j.arabjc.2011.04.013
22. W. Khalid, A. Badshah, A.-u. Khan, H. Nadeem and S. Ahmed, *Chem. Central J.*, **12**, 11 (2018); https://doi.org/10.1186/s13065-018-0378-5
23. S. Forli, R. Huey, M.E. Pique, M.F. Sanner, D.S. Goodsell, and A.J. Olson, *Nat. Protoc.*, **11**, 905 (2016); https://doi.org/10.1038/nprot.2016.051
24. O. Trott and A.J. Olson, *J. Comput. Chem.*, **31**, 455 (2010); https://doi.org/10.1002/jcc.21334
25. A.D. Hunter, *J. Chem. Educ.*, **74**, 905 (1997); https://doi.org/10.1021/ed074p905
26. N.M. O'Boyle, M. Banck, C.A. James, C. Morley, T. Vandermeersch and G.R. Hutchison, *J. Cheminform.*, **3**, 33 (2011); https://doi.org/10.1186/1758-2946-3-33
27. Z.M. Alamshany, R.R. Khattab, N.A. Hassan, A.A. El-Sayed, M.A. Tantawy, A. Mostafa and A.A. Hassan, *Molecules*, **28**, 739 (2023); https://doi.org/10.3390/molecules28020739
28. P. Bhardwaj, G.P. Biswas, N. Mahata, S. Ghanta and B. Bhunia, *Chemosphere*, **293**, 133550 (2022); https://doi.org/10.1016/j.chemosphere.2022.133550
29. L.G. Sarbu, I. Rosca and M.L. Birsa, *Antibiotics*, **14**, 307 (2025); https://doi.org/10.3390/antibiotics14030307
30. M.A. Sa'ad, R. Kavitha, S. Fuloria, N.K. Fuloria, M. Ravichandran and P. Lalitha, *Antibiotics*, **11**, 207 (2022); https://doi.org/10.3390/antibiotics11020207
31. F. Madeddu, J. Di Martino, M. Pieroni, D. Del Buono, P. Bottoni, L. Botta, T. Castrignanò and R. Saladino, *Int. J. Mol. Sci.*, **23**, 14652 (2022); https://doi.org/10.3390/ijms232314652
32. S.V. Bhuvaneshwari, A.M. Mallikarjunaswamy, K. Gouthami, S. Sekharappa and V. Nair, *Indian J. Chem.*, **63**, 1155 (2024); https://doi.org/10.56042/ijc.v63i11.13328
33. D.A. Milenković, D.S. Dimić, E.H. Avdović and Z.S. Marković, *RSC Adv.*, **10**, 35099 (2020); https://doi.org/10.1039/D0RA07062A
34. R.F. Muslim, H.M. Tawfeeq, M.N. Owaid and O.H. Abid, *Acta Pharm. Sci.*., **56**, 39 (2018); https://doi.org/10.23893/1307-2080.APS.05610
35. S. Matam, P. Kaliyan, P. Sethuramasamy and S.P. Muthu, *Asian J. Green Chem.*, **3**, 508 (2019); https://doi.org/10.33945/SAMI/AJGC/2019.4.7
36. K.B. Gangurde, R.A. More, V.A. Adole and D.S. Ghotekar, *Results Chem.*, **7**, 101380 (2024); https://doi.org/10.1016/j.rechem.2024.101380